Progress in Neurobiology 219 (2022) 102364

Contents lists available at ScienceDirect

Progress in Neurobiology

journal homepage: www.elsevier.com/locate/pneurobio

Chemogenetic stimulation of adult neurogenesis, and not neonatal neurogenesis, is sufficient to improve long-term memory accuracy

Marie Lods [a], Pierre Mortessagne [a], Emilie Pacary [a], Geoffrey Terral [b], Fanny Farrugia [a], Wilfrid Mazier [c], Nuria Masachs [a], Vanessa Charrier [a], Daniela Cota [c], Guillaume Ferreira [d], Djoher Nora Abrous [a,1,*], Sophie Tronel [a,1,*]

[a] Univ. Bordeaux, INSERM, Magendie, U1215, Neurogenesis and Pathophysiology Group, F-3300 Bordeaux, France
[b] Univ. Bordeaux, INSERM, Magendie, U1215, Endocannabinoids and Neuroadaptation Group, F-3300 Bordeaux, France
[c] Univ. Bordeaux, INSERM, Magendie, U1215, Energy Balance and Obesity Group, F-3300 Bordeaux, France
[d] Univ. Bordeaux, INRAE, Bordeaux INP, NutriNeurO, UMR 1286, Nutrition and Integrative Neurobiology Group, F-3300 Bordeaux, France

ARTICLE INFO

Keywords:
Adult neurogenesis
Hippocampus
Memory
Chemogenetic

ABSTRACT

Hippocampal adult neurogenesis is involved in many memory processes from learning, to remembering and forgetting. However, whether or not the stimulation of adult neurogenesis is a sufficient condition to improve memory performance remains unclear. Here, we developed and validated, using ex-vivo electrophysiology, a chemogenetic approach that combines selective tagging and activation of discrete adult-born neuron populations. Then we demonstrated that, in rats, this activation can improve accuracy and strength of remote memory. These results show that stimulation of adult-born neuron activity can counteract the natural fading of memory traces that occurs with the passage of time. This opens up new avenues for treating memory problems that may arise over time.

1. Introduction

The role of the dentate gyrus (DG) in memory retrieval has been extensively studied but yet its involvement in this process remains controversial. Many studies have shown that the activation of DG granule cells declines over time during consolidation and that memory retrieval is supported by reactivation of CA3 and CA1 networks (Kitamura et al., 2017; Pignatelli et al., 2019; Tayler et al., 2013), suggesting that dentate granule cells are not required for memory retrieval (Madroñal et al., 2016). However artificial reactivation of the granule cells that encoded the learning experience triggers memory retrieval (Ryan et al., 2015). It has also been shown that, in the DG, granule encoding-neurons are functionally distinct and that different neuronal ensembles are involved in different memory functions (Sun et al., 2020). Therefore, it is relevant to consider the heterogeneity of the structure when investigating its function. A cardinal feature of the DG is that it hosts adult neurogenesis as new neurons are continuously generated throughout life. Because the hippocampus is critical for memory, many studies have been devoted to understanding the role of adult neurogenesis in memory processes (Abrous et al., 2021a; Deng et al., 2010; Goncalves et al., 2016; Miller and Sahay, 2019). Manipulating adult neurogenesis impacts hippocampal-dependent learning, in particular spatial navigation (Dupret et al., 2007) and contextual fear conditioning (Gu et al., 2012). Similarly, adult neurogenesis seems to be essential to maintain spatial and contextual memory traces as ablation of adult-born neurons disrupts memory retrieval (Arruda-Carvalho et al., 2011). However, relatively few studies have shown any beneficial effect on memory resulting from the stimulation of adult neurogenesis other than those resulting from the genetic enhancement of the neurogenic pool (Berdugo-Vega et al., 2020; Sahay et al., 2011). Because it is known that adult neurogenesis is homeostatically regulated (Dupret et al., 2007), the addition of new neurons can lead to compensatory mechanisms (McAvoy et al., 2016). Thus, knowledge about the effect of specifically activating a given population of new neurons, already present at the time of learning, on subsequent memory processes is lacking.

Furthermore, the respective role of adult-born neurons and neonatally generated granule neurons seems to differ according to the memory process investigated. We have previously shown that, in contrast to

* Corresponding authors.
E-mail addresses: Nora.abrous@inserm.fr (D.N. Abrous), sophie.tronel@inserm.fr (S. Tronel).
[1] These authors contributed equally.

https://doi.org/10.1016/j.pneurobio.2022.102364
Received 19 April 2022; Received in revised form 21 September 2022; Accepted 6 October 2022
Available online 13 October 2022

adult-born neurons, neonatally generated ones are not activated by spatial learning (Tronel et al., 2015b) nor by spatial memory retrieval (Lods et al., 2021) and that they are not necessary for memory stabilization (Masachs et al., 2021). In addition, adult-born neurons may have a greater impact on behavior and make unique contributions to hippocampal functioning since they are more plastic than the neurons generated during development (Cole et al., 2020; Lodge and Bischofberger, 2019). Therefore, investigating the specific role of adult neurogenesis in memory retrieval could bring new information to the understanding of memory maintenance. In order to address these issues, we tested whether chemogenetic stimulation of neuronal activity of new neurons during retrieval could enhance long-term memory retention in two different hippocampal-dependent tasks.

2. Methods

2.1. Animals

A total of 154 male Sprague–Dawley rats (OFA, Charles Rivers, France) were used for these experiments. Rats weighing between 250 and 275 g (2 months of age) at time of delivery were individually housed in standard cages under a 12/12 h light/dark cycle with ad libitum access to food and water.

Pregnant female (n = 13, three month-old, 240–260 g body weight on delivery) Sprague–Dawley rats (OFA, Charles Rivers, France) were individually housed in plastic breeding cages under standard laboratory conditions. After birth, only litters of 8–11 pups with approximately equal sex ratios were retained for the study. The litters were raised by their biological mothers until weaning (21 days after birth). After weaning, only the male progeny were kept, and animals were randomly assigned to the different experimental groups.

All experiments were performed in accordance with the recommendations of the European Union (2010/63/UE) and were approved by the ethical committee of the University of Bordeaux (#Dir1367, #17467, #22698).

2.2. Plasmids and retroviruses

The Gs DREADD was cloned by PCR using pcDNA5/FRT-HA-rM3D (Gs) (Addgene #45549; (Armbruster and Brandeau, 2007)) as a template (See Table S2 for PCR primers) and then inserted into the *Bam*HI site of a CAG-IRES-GFP retroviral backbone (Jessberger et al., 2008). The resulting construct CAG-Gs-IRES-GFP was sequenced using specific primers (Table S2) and is named Gs-GFP-RV in the text. The control construct had the same viral backbone without the insert (GFP-RV in the text).

High titers of retroviruses were prepared with a human 293-derived retroviral packaging cell line (293GPG) (Ory et al., 1996), kindly provided by Dr Dieter Chichung Lie (University of Erlangen-Nuremberg). Virus-containing supernatant was harvested three days after transfection with Lipofectamine 2000 (Invitrogen, Oregon, US. #11668–019). This supernatant was then cleared from cell debris by centrifugation at 2191 g for 15 min and filtered through a 0.45 μm filter (Millipore, Massachusetts, US). Viruses were concentrated by two rounds of centrifugation (respectively 46,000*g* and 67,629*g*, 1 h each) and resuspended in PBS.

2.3. Retroviral injections

Adult rats were anaesthetized with 3% isoflurane and placed in the stereotaxic frame, where they were maintained on 2% isoflurane for the duration of the surgery. Analgesia was provided by a subcutaneous injection of Metacam (1 mg/Kg). Retroviruses were stereotaxically injected (2 μL per injection site at 0.3 μL/min) into the dentate gyrus of adult rats with a microcapillary pipette connected to a micro-syringe pump (KDScientific SPLG130) attached to the stereotaxic frame. To check the efficiency of the virus in vivo and the effect on the survival of new neurons, two bilateral injections were made into the Hilus of the dorsal hippocampus through stereotaxic surgery coordinates from Bregma (−3.2 mm posterior, ± 1.6 mm lateral, −4.2 ventral). Four bilateral injections were made for behavioral and electrophysiological experiments (−3.2 mm posterior, ± 1.6 mm lateral, −4.2 ventral; and −3.8 mm posterior, ± 1.8 mm lateral, −4.2 mm ventral according to the Paxinos and Watson atlas).

Rats from postnatal day 3 were anaesthetized on ice and placed on a neonatal rat adapter in the stereotaxic frame. They were maintained on ice during the surgery. Retroviruses were bilaterally injected (1 μL per injection site at 0.3 μL/min) into the dentate gyrus of with a microcapillary pipette (from Bregma: −1.2 mm posterior, ± 1.3 mm lateral, −2.6 ventral). At the end of the experiment, only rats with labeled-cells in both hemispheres were kept in the analysis.

2.4. BrdU injection

BrdU (5-bromo-2′-deoxyuridine, Sigma-Aldrich, Missouri, US) was dissolved in a Phosphate Buffer (pH 8.4) and rats received one injection (100 mg/kg) intra-peritoneally (ip).

2.5. Water maze procedures

The apparatus consisted of a circular plastic swimming pool (180 cm diameter, 60 cm height) that was filled with water (20 ± 1 °C), rendered opaque by the addition of a white cosmetic adjuvant. Two days before training, the animals were habituated to the pool for one minute. During training, animals were required to locate a submerged platform (16 cm diameter) hidden 1.5 cm under the surface of the water in a fixed location, using the spatial cues available within the room. All rats were trained for four trials per day (90 s with an inter-trial interval of 30 s, with release from one of three starting points selected in a pseudo-random sequence each day) during 6 days. If an animal failed to locate the platform itself, it was placed on the platform by the experimenter at the end of the trial. The time to reach the platform was recorded with a video camera that was fixed to the ceiling of the room and connected to a computerized tracking system (Videotrack, Viewpoint, Lyon, France) located in an adjacent room.

Four weeks after learning, rats were submitted to a retention test in the water maze. During the test, rats were put in the water maze for 60 s in the absence of the platform. Performances were assessed using several parameters: the amount of time spent in and number of entries (annulus crossing) into each zone. Zones were defined as a 15 cm radius (corresponding to 2.8% of pool surface (Moser et al., 1998)) around the center of the original platform location (Target zone; T) and the three equivalent areas in each of the other quadrants (other zones; O). The discrimination ratio for comparing data in the target zone and data in the other zones was calculated as follows: ((T-O)/(T + O)). The grouped heat-maps were created with Ethovision XT 10, Noldus (Nantes, France). The color of a pixel represents the average proportion of a track that is found at that location. We also calculated the Gallagher proximity index (Gallagher et al., 1993) to estimate the search paths corresponding to the average distance of rats from the former platform. This measure was obtained by sampling the position of the animal in the maze (25 times per second) to provide a record of its distance from the escape platform in 1 s averages.

2.6. Contextual fear conditioning

The fear conditioning chamber consisted of a squared conditioning chamber (30 cm × 30 cm X 40 cm) of a brightness of 10 lux, containing a stainless steel grid floor (Imetronic, Marcheprime, France). Rats were habituated to handling for 3 days before conditioning. On conditioning day, rats were placed in the chamber for 2 min for habituation. Then they received 2 foot-shocks (0.8 mA each, 1 s) 60 s apart (wait 1) and

they were left undisturbed for another 60 s period (wait 2). Chambers were cleaned with 70% ethanol between each rat. On testing day, rats were placed in the chamber for 3 min. In the second fear conditioning experiment, rats were tested in context A (conditioning chamber) or in context B (novel odor, lighting, cage floor, and visual cues). Half of the rats were tested in context A and 48 h later in context B, the other half was first tested in B and then in A. Behavioral data were automatically collected using infrared beams spaced 1 cm apart in the x and y planes, located at the floor of the chambers. Freezing behavior was measured following the cessation of movement for at least 2 s

2.7. CNO delivery

The DREADD ligand CNO (Clozapin-n-Oxyde, Hello Bio,# HB6149) was dissolved in a saline solution and delivered via one ip injection of 1 mg/kg in rats 60 min before the test.

2.8. Immunohistochemistry and analysis

Animals were perfused transcardially with a phosphate-buffered solution of 4% paraformaldehyde. After one week of fixation, brains were cut with a vibratome. Free-floating 50 μm thick sections were processed according to a standard immunohistochemical procedure to visualize GFP (Chicken primary antibody, 1:2000, Abcam, Cambridge, UK. #Ab13970), BrdU (Mouse primary anitobody, 1:200, Dako Agilent, Santa Clara, US. #M0744), and Zif268 (Rabbit primary antibody, 1:500, Santa Cruz Biotechnology, Santa Cruz, US. #SC-189) on alternate1-in-10 sections.

GFP positive cells throughout the entire dentate gyrus were revealed using the biotin-streptavidin technique (ABC kit, Vector Labs, Peterborough, UK #PK-4000) and 3,3′-diaminobenzidine as a chromogen with a biotinylated goat anti chicken antibody (1:500, Jackson ImmunoResearch, Cambridgeshire, UK. #103–065–155).

GFP-IR cells were counted under a 100x microscope objective throughout the entire septo-temporal axis of the granule and subgranular layers of the dentate gyrus (DG). The total number of cells was estimated using the optical fractionator method, and the resulting numbers were tallied and multiplied by the inverse of the sections sampling fraction (1/ssf10).

BrdU-positive cells throughout the entire granular layer of the supragranular and infragranular blades of the DG were revealed using the biotin-streptavidin technique with a horse anti-mouse antibody (1:200, Vector Labs, Peterborough, UK. #BA-2001). The total number of cells was counted under a 100x microscope objective throughout the entire left septo-temporal axis of the granule and subgranular layers of the DG as previously described (Tronel et al., 2010a). The total number of cells was estimated using the optical fractionator method.

To estimate the density of Zif268-IR cells (both sides), two-dimensional images of the entire dentate gyrus were acquired with a slide scanner. The slide scanner was a Nanozoomer 2.0HT with a fluorescence imaging module (Hamamatsu Photonics France) using an objective UPS APO 20X NA 0.75 combined to an additional lens 1.75X, leading to a final magnification of 35X. Virtual slides were acquired with a TDI-3CCD camera. Zif268-IR cells were counted by using QuPath sofware. The results are expressed as the number of IR cells per mm^2 of the granule cell layer (GCL) of the DG.

Activation of GFP-IR neurons was examined by immunohistofluorescence. GFP was visualized with an Alexa-488 goat anti-chicken antibody (1:1000, Invitrogen, Oregon, US. #A-11039). In the same sections, $Zif268^+$ cells was visualized with an Alexa-568 goat anti-rabbit antibody (1:1000 Invitrogen, Oregon, US. #A-11011). Double labeling was determined by using a SPE confocal system with a plane apochromatic 63X oil lens (digital zoom of 2). The percentage of GFP cells expressing Zif268 was calculated as follows: (Nb of GFP^+-$Zif268^+$ cells)/(Nb of GFP^+-$Zif268^-$ cells + Nb of GFP^+-$Zif268^+$ cells) x 100. For the representative image of Gs-retrovirus GFP fluorescence, nuclei in the dentate gyrus were revealed using DAPI (1:10,000, Invitrogen, Oregon, US. #P36931). Mosaic pictures were taken using an SP8 confocal system with a 20X multi-immersion lens (digital zoom of 1.2).

2.9. Electrophysiological recordings

Infected animals were deeply anesthetized (167 mg/Kg ketamine and 16,7 mg/Kg xylazine) and sacrificed. Dissected brain was immediately immerged in ice-cold oxygenated cutting solution (in mM: 180 Sucrose, 26 NaHCO3, 11 Glucose, 2.5 KCl, 1.25 NaH2PO4, 12 MgSO4, 0.2 CaCl2, saturated with 95% O2–5% CO2). 350 μm slices were obtained using a vibratome (VT1200S Leica, Germany) and transferred into a 34 °C bath of oxygenated aCSF (in mM: 123 NaCl, 26 NaHCO3, 11 Glucose, 2.5 KCl, 1.25 NaH2PO4, 1.3 MgSO4, 2.5 CaCl2; osmolarity 310 mOsm/l, pH 7.4) for 30 min and then cooled down progressively till room temperature (RT; 23–25 °C). After a 45 min recovery period at RT, slices were anchored with platinum wire at the bottom of the recording chamber and continuously bathed in oxygenated aCSF (RT; 2 ML/min) during recording.

Infected newborn granule cells were identified using GFP with a fluorescence/infrared light (pE-2 CoolLED excitation system, UK). Neuron action potential firing was monitored in whole-cell current-clamp recording configuration. Patch electrodes were pulled (micropipette puller P-97, Sutter instrument, USA) from borosilicate glass (O.D. 1.5 mm, I.D. 0.86 mm, Sutter Instrument) to a resistance of 2–4 mΩ. The pipette internal solution contained [in mM: 125 potassium gluconate, 5 KCl, 10 Hepes, 0.6 EGTA, 2 MgCl2, 7 Phosphocreatine, 3 adenosine-5′-triphosphate (magnesium salt), 0.3 guanosine-5′-triphosphate (sodium salt) (pH adjusted to 7.25 with KOH; osmolarity 300 mOsm/l adjusted with D-Mannitol)] as well as biocytin 0.4% (a liquid junction potential of −14.8 mV was corrected for in the data and statistics). In order to test the effect of CNO on IP firing, neurons were clamped with positive currents until reaching low excitable potential (AP frequency<2 Hz). It should be noted that the current injected was no different between control GFP-RV and Gs-GFP-RV infected cells (t_{10} =1.078; p = 0,31).

CNO (10 μM in aCSF) was fast perfused close to the recording cell for 30 s then immediately washed out. Electrophysiological data were recorded using a Multiclamp 700B amplifier (Molecular devices, UK), low-pass filtered at 4 kHz and digitized at 10 Hz (current clamp) or 4 Hz (voltage clamp) (Digidata 1440 A, Molecular devices, UK). Signals were analyzed offline (Clampfit software, pClamp 10, Molecular devices, UK). For statistical analysis, “Vehicle” data were collected during the last 60 s before CNO perfusion, then “CNO” data were collected after 45 s of CNO treatment.

2.10. Statistical analysis

The data (mean±SEM) were analyzed using the Student t-test (two-tailed) and two ways ANOVA which was followed by the Tukey’-comparison test when necessary. All analyses were carried out using the software GraphPad Prisms 6 and 9.

3. Results

We first wanted to analyze long-term spatial memory in the water maze (WM). Towards this end, 2 months-old adult rats were trained to locate a hidden platform in a fixed location in the water maze (WM) for 6 days. Then two groups of animals were tested respectively 48 h or 4 weeks later to evaluate recent and remote memory respectively (Fig. 1a). To do so, the platform was removed and the strength and accuracy of memory were measured by evaluating the search around the position of where the platform was located (target zone). The results showed that, at both tests, rats remembered the position of the platform since latency to cross the position of where the platform was during training and the distance traveled to this position were not different between groups and latency was not different from the latency on the

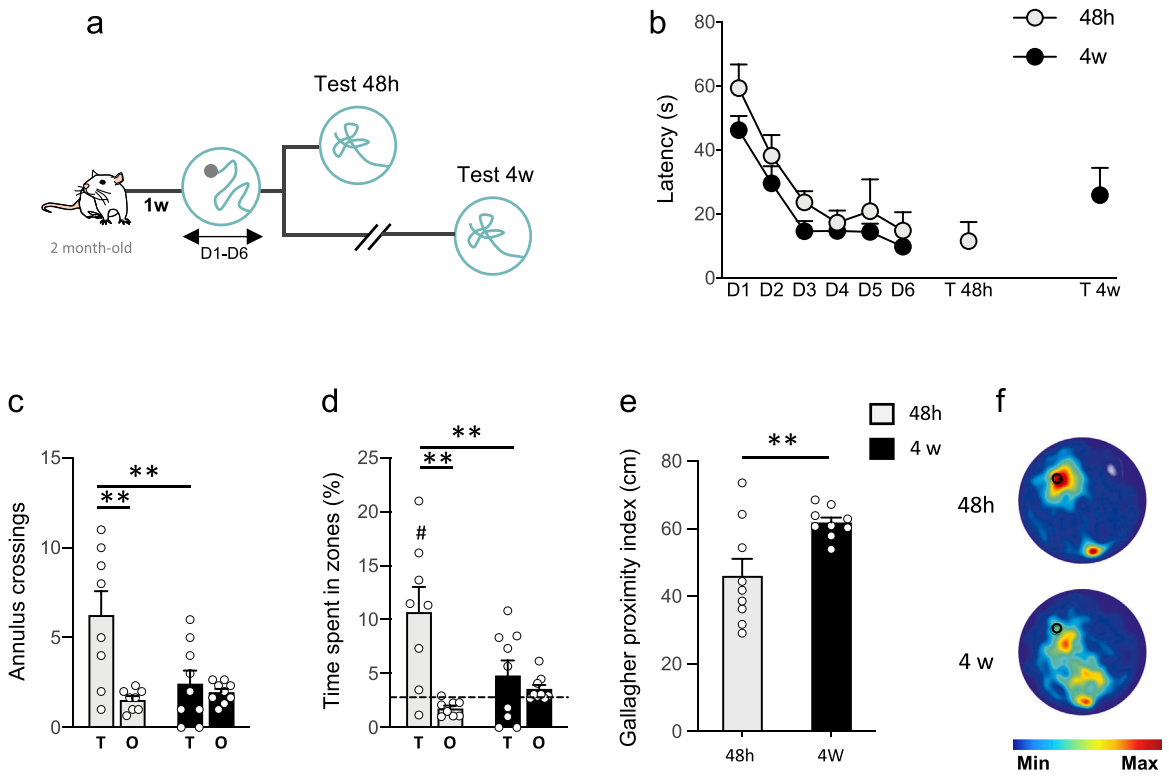

Fig. 1. Long-term memory retention four weeks after learning. a – Two-month-old adult rats were trained in the WM for 6 days. One group of rats (n = 8) was submitted to a probe test 48 h after training and another group of rats (n = 9) was tested 4 weeks after training. b – Latency to reach the platform during learning and to first cross the position of the platform during the tests. There was no difference between groups at learning and the latency to reach the platform position was similar at 48 h or 4 weeks after training. c – Number of annulus crossings (zone entries), animals show a significant preference for the target zone (T) compared to the other zones (O) when tested 48 h after training whereas no difference was observed at the 4w test (zone X group interaction: $F(1,15)= 7.73$; $p = 0.014$; zone effect: $F(1,15)= 11.66$; $p = 0.0038$; group effect: $F(1,15)= 5.23$; $p = 0.037$) d – Percentage of time spent in the target zone compared to that of the other zones. Rats that were tested 48 h after training spent significantly more time in the target zone compared to the other zones and the amount of time was higher than that of chance level (dash line). No difference was observed when animals were tested 4 weeks after training (zone X group interaction: $F(1,15)= 7.14$; $p = 0.017$; zone effect: $F(1,15)= 12.60$; $p = 0.0029$; group effect: $F(1,15)= 2.76$; $p = 0.12$) e- Gallagher proximity index. Search paths were closer to the former platform at 48 h compared to those at 4w (t_{16} =3.003; $p = 0.0084$). (**$p < 0.01$; # $p < 0.05$ compared to chance level). f - Density plot for grouped data: The color level represents the lowest to the highest location frequency in pixels. All data shown are mean ± s.e.m. For statistical details, see Table S1.

last training day (Figs. 1b, S1a). However, when we considered the number of annulus crossings (Fig. 1c) or the percentage of time spent in the target zone (Fig. 1d), results showed that the performances were impaired when rats were tested 4 weeks after training. Both annulus crossings and time spent in zone were higher in the target zone compared to those in the other zones at 48 h, whereas generally no difference was observed when memory was tested at 4 weeks (Figs. 1c-e; S1b-e). In order to obtain another measure of spatial performance accuracy, we calculated the Gallagher proximity index (Gallagher et al., 1993), which revealed that the search paths were closer to the target platform at 48 h compared to those at 4 weeks This demonstrates that some spatial information was retained at both delays (as evidenced by latency and distance traveled to platform) but that the passage of time disrupted some parameters indicative of spatial memory accuracy.

We then hypothesized that the stimulation of adult-born neurons could improve memory accuracy. With this aim in mind, we developed a GFP retrovirus (RV) into which we inserted a DREADD-(Designer Receptors exclusively Activated by Designer Drug)Gs construct (Gs-GFP-RV)(see Suppl Methods). This tool acts initially by infecting new granule cells at their birth. Several weeks later, when they are fully integrated into the network, these same cells can then be activated upon binding of the synthetic ligand Clozapine-N-Oxide (CNO). To ensure that Gs-GFP-RV injections into the dentate gyrus (DG) had no impact on new neuron survival, rats were injected in the DG with either the Gs-GFP-RV or with a control retrovirus (GFP-RV). At the same time, both groups of animals were injected with bromodeoxyuridine (BrdU) to study cell genesis. Six weeks later, the animals were sacrificed in order to quantify the number of surviving BrdU-positive cells. No differences were observed between the groups, demonstrating that injection of the Gs-GFP-RV has no impact on BrdU-labeled cell survival (Fig. 2a-b). To further confirm that CNO injections specifically activate Gs-GFP-RV cells, rats were injected with Gs-GFP-RV in the left DG and with a control GFP-RV in the right DG. Six weeks later, all animals received an intraperitoneal (IP) injection of CNO (1 mg/Kg) and were sacrificed two hours later (Fig. 2c). We determined the activation of the infected cells by analyzing the expression of the immediate early gene Zif268 in the GFP labeled cells. We found that 98.8% of the cells infected with the Gs-GFP-RV were activated by CNO compared to 1.7% of the cells injected with a Ctrl-retrovirus (Fig. 2d). By analyzing the density of Zif268-IR cells, we found that there was no difference between the left and right GCL infected with Gs-GFP-RV and the control GFP-RV, demonstrating that the stimulation of Gs-GFP transduced neurons did not influence the overall activity of the principal neurons of the DG (Fig. 2e). Finally, we performed whole cell recordings of Gs-GFP-RV or control GFP-RV-infected cells (Fig. 2f) and assessed changes in cell excitability after CNO application (Fig. 2g). Local perfusion of CNO quickly and reversibly enhanced Gs-GFP-RV-infected cell excitability, which was seen by an increase in both resting potential (RP) and action potential (AP) firing rate (Fig. 2h). No such effect was seen in GFP-RV-infected cell excitability (Fig. 2i). It should be noted that both the RP and the AP of the GFP-RV infected cells and the Gs-GFP-RV infected cells were similar before the CNO application (Veh in Fig g,h; RP: t_{10} =1.93, $p = 0.08$ and

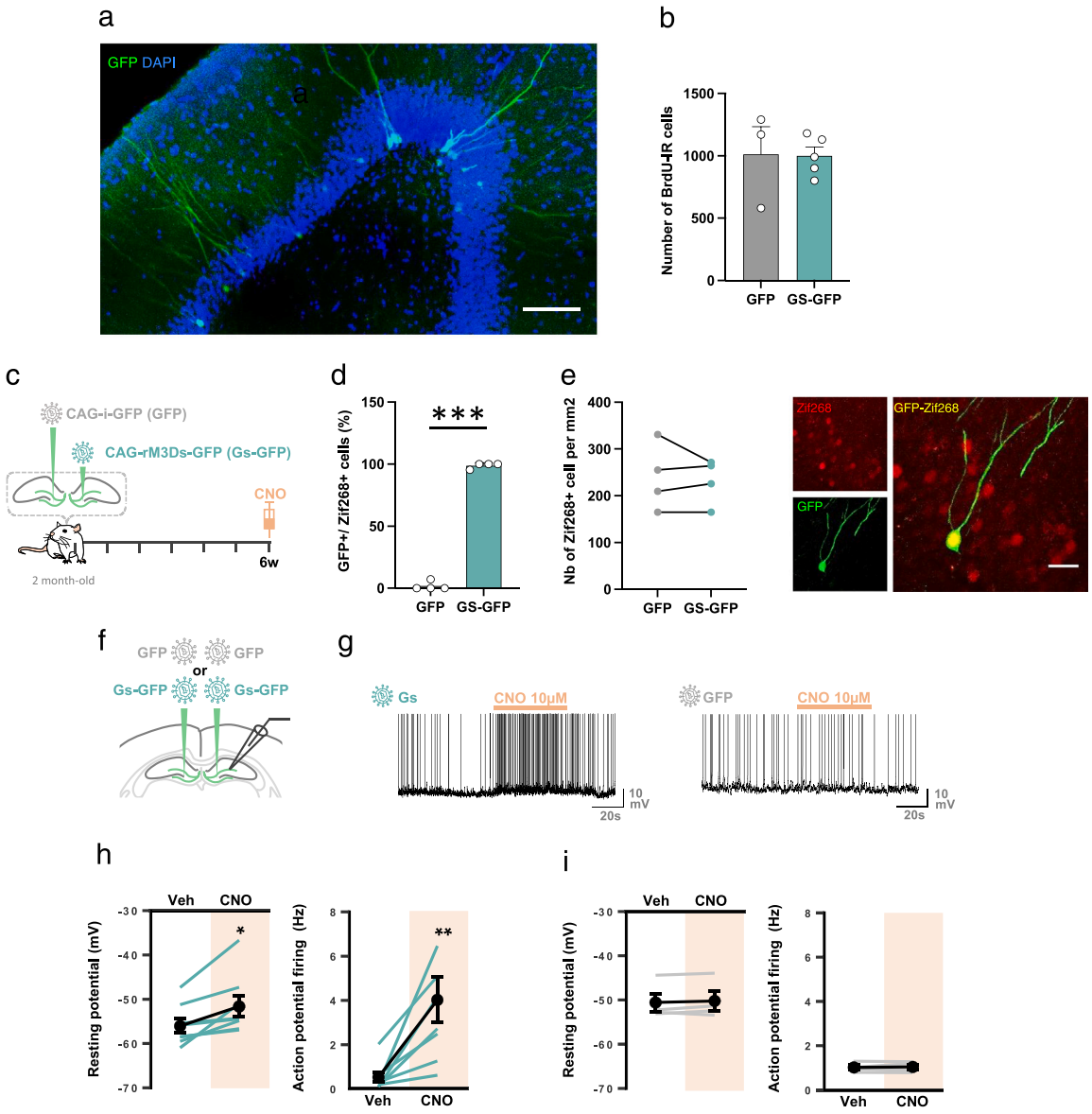

Fig. 2. Stimulation of Gs-GFP-RV is efficient in vitro and in vivo. a – GFP fluorescence in DG labeled neurons 6 weeks post-injection of the Gs-GFP-RV (scale: 100 µm). b – Injection of retroviruses does not impact the survival of new neurons 6 weeks post-injection (t_6 =0.07, P = 0.94; unpaired *t*-test; n = 3 GFP- and n = 5 Gs-GFP- rats). c – GFP and Gs-GFP retroviruses were injected in the left and right DG, respectively, of adult rats. Six weeks later, rats were injected with CNO (IP, 1 mg/Kg) and sacrificed 2 h later. d - CNO Injection strongly enhances Gs-GFP cell activation in vivo compared to GFP cells. (t_3 =54.90; *** $P < 0.0001$; Paired *t*-test; n = 4 rats). e- Total zif268 activation in each hemisphere (t_6 =0.1971, P = 0.8503; unpaired *t*-test. *Right:* Illustration of a Gs-GFP cell (green) expressing Zif268 (red) (scale: 20 µm). f – Scheme for whole-cell recording from Gs-GFP or GFP cells in the DG. g - Representative traces of 10 µM CNO perfusion effect onto cellular activity. CNO is inert in GFP cells, but quickly and reversibly enhances Gs-GFP cell activity. h - CNO depolarizes Gs-GFP cells and increases their action potential firing. Blue lines represent data from individual cells, black lines are the mean of the blue lines. [Paired *t*-tests, Vehicle vs CNO treated rats. Resting potential (t_7 =3.22; * $P = 0.015$); Action potential firing (t_7 =3.51; ** $P = 0.010$; n = 2 rats and 8 cells)]. i - CNO has no effect on resting potential and action potential firing frequency of GFP cells. Gray lines represent data from individual cells, black lines are the mean of the gray lines. [Paired *t*-tests, Vehicle vs CNO applied for 30 s, treated rats. Resting potential (t_3 =1.02; $P = 0.38$) Action potential firing (t_3 =0.42; $P = 0.70$; n = 3 rats and 4 cells)]. All data shown are mean ± s.e.m. For statistical details, see Table S1.

AP firing t_{10} =1.43, p = 0.18). Similarly, the excitability and the intrinsic electrophysiological properties were not altered in Gs-GFP-RV infected cells (see Methods; Control vs Gs: resting potential, −68 ± 1.73 mV vs −73.9 ± 2.25 mV, t_{10} =1.7; p = 0.12; capacitance, 43.8 ± 4.8 pF vs 38.3 ± 7.3 pF, t_{10} =0.5; p = 0.63; membrane resistance 115.5 ± 11.4 MOhm vs 160.1 ± 46.7 MOhm, t_{10} =0.65; p = 0.53; unpaired t test, data not shown).

Since memory fades with the passage of time, we then sought to determine whether stimulating adult-born neurons during retrieval could improve memory accuracy. We have recently shown that adult-born neurons that were immature (1 week-old) or mature (6 weeks-old) at the time of training were both activated by remote memory retrieval (Lods et al., 2021). We first focused on the population of neurons born one week before training (Fig. 3a). We have previously shown that the survival and dendritic development of this latter population is increased by spatial learning (Tronel et al., 2010a) and it has been hypothesized that these immature neurons could be primed by experience (Alvarez et al., 2016). More recently, we showed that this immature population is required for maintaining the memory trace after remote retrieval (Lods et al., 2021). However, whether the stimulation of neurons that were immature at the time of learning is capable of improving memory retrieval is not known. Two month-old rats were

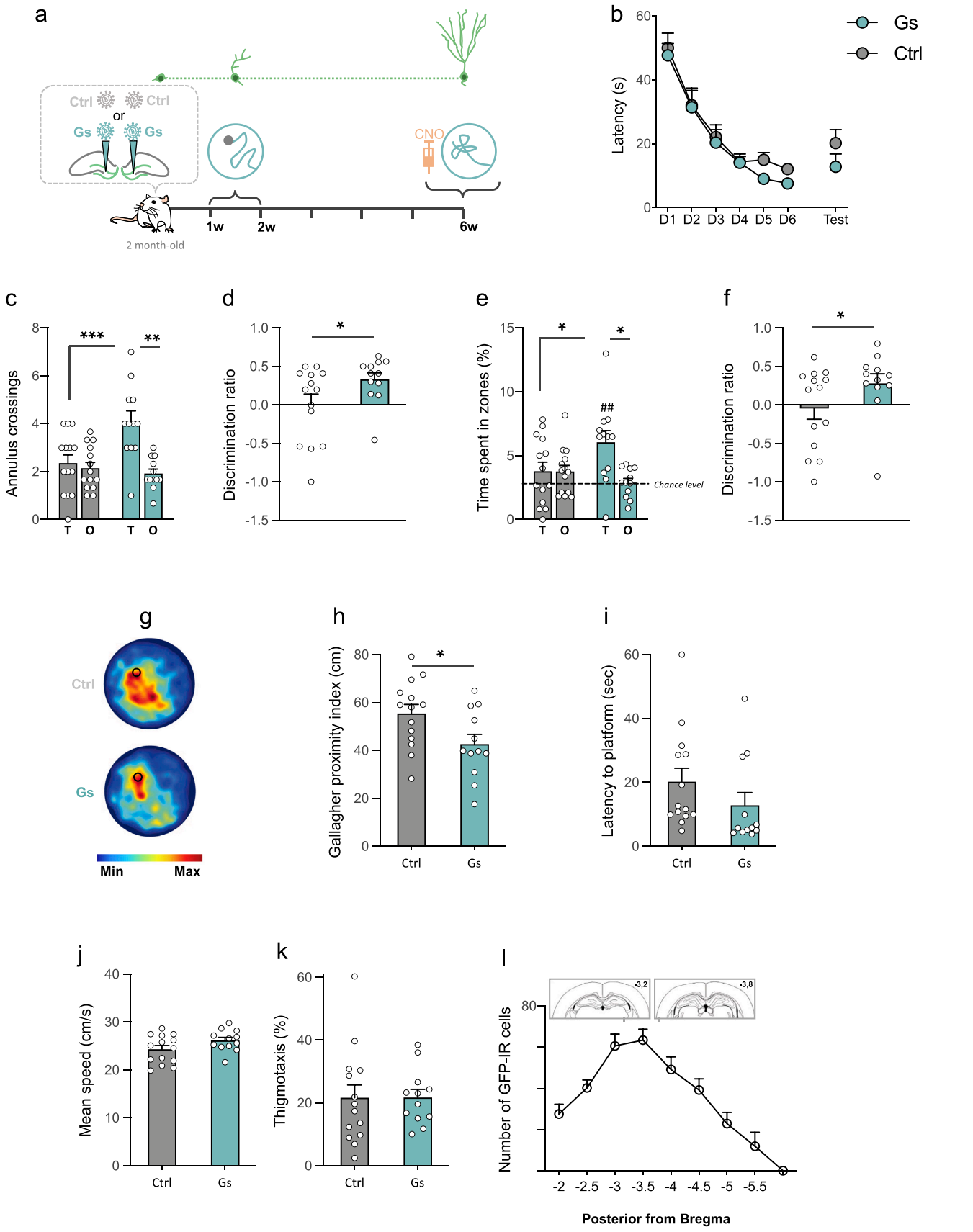

(caption on next page)

Fig. 3. Chemogenetic stimulation, during remote retention test, of adult-born neurons that were immature at the time of learning enhances memory accuracy. a - Timeline of behavioral procedure with water maze training 1 week after retrovirus injections (Gs-GFP-RV rats, n = 12; GFP-RV rats, n = 14) and retention test four weeks after training. CNO was injected 1 h before the test. b - Latency to find the hidden platform: For all groups, latency decreases over time during training and no difference was observed at the retention test. c – Number of annulus crossings during test: Gs-GFP-RV rats entered more in the target zone that in the other zones whereas no difference was observed in GFP rats (zone X group interaction: $F(1,24)= 6.90$; $p = 0.0148$; zone effect: $F(1,24)= 10.26$; $p = 0.0038$; group effect: $F(1,24)= 8.37$; $p = 0.008$). d – Discrimination ratio of annulus crossings for Ctrl and Gs ($t_{24} =1.987$;$p = 0,0292$). e – Gs-GFP-RV rats spend more time in the target zone compared to GFP-RV rats. For Gs-GFP rats, the time spent was significantly higher in the target zone compared to that in the other zone and higher than the chance level (dash line) (zone X group interaction: $F(1,24)= 4.33$; $p = 0.048$; zone effect: $F(1,24)= 4.46$; $p = 0.045$; group effect: $F(1,24)= 1.92$; $p = 0.18$). f – Discrimination ratio for time spent in zones for Ctrl and Gs ($t_{24} =1.715$;$p = 0,0496$). g - Density plot for grouped data: The black circle represents the position of the platform during training. The color level represents the lowest to the highest location frequency in pixels. h – Gallagher proximity index. Search paths were closer to the former platform for The Gs-GFP rats compared to those of control GFP rats ($t_{24} =2.31$; $P = 0.03$). i – Latency to cross the platform position. There was no difference between groups. j – Mean Speed of swimming. There was no difference between groups. k – Thigmotaxic behavior. There was no difference between groups. l– Number of GFP-IR in the DG on alternate 1-in-10 50 μm sections. The retrovirus infection spreads at least 4 mm across the septotemporal dentate gyrus axis, illustrations on top of the graph represent the sites of injections. (*$p < 0.05$; ## $p < 0.01$ compared to chance level). All data shown are mean ± s.e.m. For statistical details, see Table S1.

injected with either the Gs-GFP-RV or the GFP-RV. One week later, these rats were trained in the WM (Fig. 3a). All rats learned to find the platform (Fig. 3b). Four weeks after training, we performed a remote retention test, one hour prior to which all rats received an IP injection of CNO. We found that stimulation of this population enhanced memory retention. Compared to GFP rats, the number of annulus crossings and the time spent in the target zone were higher in the Gs-GFP rats (Figs. 3c-g; S2a-d). Gs-GFP, but not GFP, rats showed also a clear preference for the target zone compared to the others zones with performances significantly above the chance level. These results were confirmed by calculating a discrimination ratio between the target zone and the others zones for both groups and for both the number of annulus crossings (Fig. 3d) and the time spent in zones (Fig. 3f). The Gallagher proximity index revealed that the search paths were closer to the target platform for the Gs-GFP rats compared to those of control GFP rats (Fig. 3h). Additional analyses did not reveal any group differences for the latency to cross the platform position, the mean speed, and the thigmotaxis (Fig. 3i–k). These results demonstrate that stimulation of adult-born neurons that were immature at the time of learning could enhance remote memory accuracy. To confirm that dentate granule neurons were correctly transduced, the number of GFP positive cells was estimated in the DG. This analysis showed that 3156 ± 295 cells were GFP positive and distributed along the DG septo-temporal axis (Fig. 3l). Of note, no correlation was found between the number of transduced-cells and the behavioral performances.

We then performed the same experiment, but this time, we targeted the population of adult-born neurons that were mature (6 week-old) at the time of training (Fig. 4a).

This specific population is known to be activated by spatial learning and retrieval and its pharmacological ablation disrupted spatial memory learning(Lemaire et al., 2012; Tronel et al., 2015a). We have also recently shown that chemogenetic silencing of this population impairs recent spatial memory retrieval(Lods et al., 2021). Hence, two month-old rats were injected with either the Gs-GFP-RV or the GFP-RV. Six weeks later, they were trained in the WM. All groups learned to find the platform (Fig. 4b). Four weeks after training, we performed a remote retention test, one hour prior to which all rats received an IP injection of CNO (Fig. 4a). Stimulation of mature adult-born neurons infected with the Gs-GFP-RV enhanced retention. Both Gs-GFP and GFP rats made more crossings and spent more time in the target zone compared to those in the other zones (Figs. 4c,d,e; S3a-d). The discrimination ratio reveals that the Gs-GFF rats made more crossings in the target zone compared to the other zones (Fig. 4d) but the ratio failed to reach significance for the time spent in zones (Fig. 4f). However, the search paths, as assessed using the Gallagher proximity index, were closer to the target position for the Gs-GFP rats compared to those of control GFP rats (Fig. 4g). As previously found, there was no effect of the treatment on latency to cross the platform position, mean speed or thigmotaxis (Fig. 4i-k). The neurons transduced by the Gs-GFP-RV (1303 ± 150 cells) were distributed along the DG septo-temporal axis (Fig. 4l). As previously found, there was no correlation between the number of transduced-cells and the behavioral performances.

One could argue that the stimulation of the dentate gyrus, no matter the population targeted, could enhance memory retention. To determine whether the effect observed on memory was specific to the stimulation of adult-born neurons, we targeted dentate granule neurons generated postnatally. To do so, rats were injected with either the Gs-GFP-RV or the GFP-RV, 3 days after birth (P3). Then rats were trained in the WM at 2 months of age. Four weeks later, CNO was injected one hour before a probe test (Fig. 5a). In this case, the stimulation of postnatally-generated granule neurons had no effect on memory accuracy assessed through annulus crossings, time spent in zones and Gallagher proximity index (Figs. 5b-f; S4a-d). Furthermore, latency, mean speed and thigmotaxis revealed no difference between groups (Fig. 5g-i). We estimated the number of neurons transduced by the Gs-GFP-RV and we found, as expected, that more neurons were targeted compared to what was found in previous experiments with adult-born neurons. 7588 ± 1255 cells were GFP positive and distributed along the DG septo-temporal axis (Fig. 5j). These results indicate that the beneficial memory effects of chemogenetic stimulation do not depend on the number of DG cells transduced.

Altogether these data reveal that chemogenetic stimulation of adult-born neurons generated before learning, and not neonatally-born granule neurons, enhances remote memory quality which fades with the passage of time.

We next investigated whether chemogenetic stimulation of adult-born neurons could enhance long-term memory in another hippocampal-dependent task, i.e, contextual fear conditioning (CFC). Towards this end, two month-old rats were injected with either the Gs-GFP-RV or the GFP-RV. One week later, these rats were trained in CFC (Fig. 6a). We used a classical CFC protocol dependent upon the hippocampus, established by Fanselow (2000, 1990) in which two mild foot-shocks were delivered in the conditioning context over a period of 4 min (Fig. 6b). During conditioning, both groups had the same level of freezing (Fig. 6c). Five weeks later, when the targeted cells reached the age of 6 weeks-old, we performed a remote retention test, one hour prior to which all rats received an IP injection of CNO. Freezing was measured over 180 s (Fig. 6b). The results showed the level of freezing was higher in the Gs-GFP rats compared to that of GFP control animals (Fig. 6d). Finally, we estimated the number of neurons transduced by the Gs-GFP-RV and we found that 1799 ± 311 cells were GFP positive and distributed along the DG septo-temporal axis (Fig. 6e,f).

Finally, to be sure that the increase of freezing was specific to the conditioning context, we replicated this latter experiment and rats were tested in both the conditioning context and a different context. A novel cohort of two month-old rats was injected with either the Gs-GFP-RV or the GFP-RV and trained in CFC in context A as previously described (Fig. 7a). During conditioning, both groups had the same level of freezing (Fig. 7b). Then, 5 weeks later, all rats received an IP injection of CNO one hour prior testing. Half of the rats were tested in the conditioning context A and the other half in a neutral context B. Two days

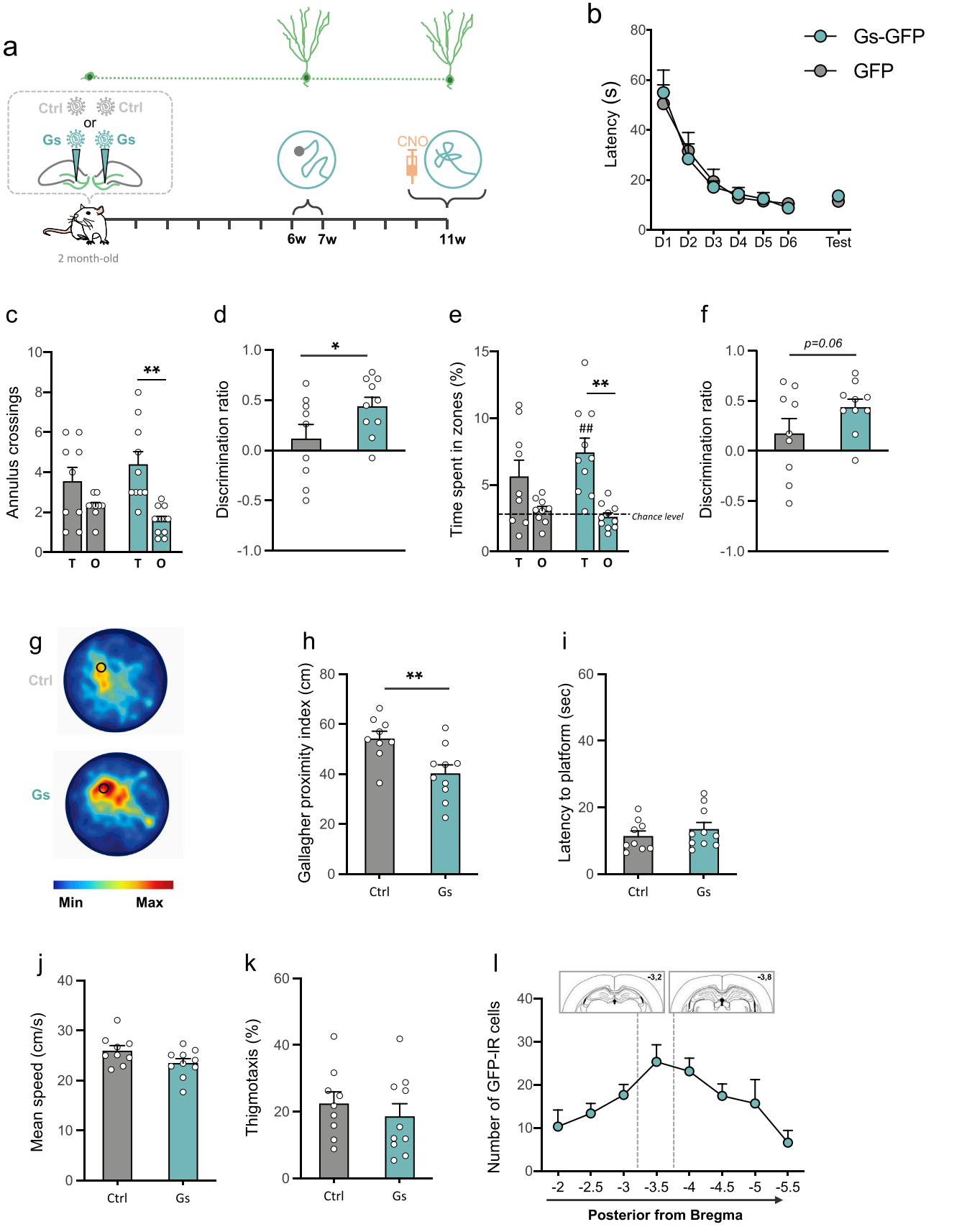

(caption on next page)

Fig. 4. Chemogenetic stimulation, during remote retention test, of adult-born neurons that were mature at the time of learning enhances memory accuracy. a - Timeline of behavioral procedure with water maze training 6 weeks after retrovirus injections (Gs-GFP-RV rats, n = 10; GFP-RV rats, n = 9) and retention test four weeks after training. CNO was injected 1 h before the test. b – Latency to find the hidden platform: For all groups, latency decreases over time during training and no difference was observed at the retention test. c – Number of annulus crossings during test: Gs-GFP-RV rats entered more in the target zone that in the other zones whereas no difference was observed in GFP rats (zone effect: F(1,17)= 14.63; p = 0.0014 and t_9 = 4.04; P = 0.0029 for Gs and t_8 = 1.54; P = 0.16 for ctrl). d – Discrimination ratio of annulus crossings for Ctrl and Gs (t_{17} =1.98;p = 0032). e –For Gs-GFP rats, the time spent was significantly higher in the target zone compared to that in the other zone and higher than the chance level (dash line, t_9 =4.31; P = 0.002) (zone effect: F(1,17)= 16.87; p = 0.0007 and t_9 = 4.16; P = 0.0025 for Gs and t_8 = 1.84; P = 0.10 for ctrl). f – Discrimination ratio for time spent in zones for Ctrl and Gs (t_{17} =1.606;p = 0,0633). g Density plot for grouped data: The black circle represents the position of the platform during training. The color level represents the lowest to the highest location frequency in pixels. h- Gallagher proximity index. Search paths were closer to the former platform for The Gs-GFP rats compared to those of control GFP rats (t_{17} =3.12; P = 0.0063). i – Latency to cross the platform position. There was no difference between groups. j – Mean Speed of swimming. There was no difference between groups. k – Thigmotaxic behavior. There was no difference between groups. l – Number of GFP-IR in the DG on alternate 1-in-10 50 μm sections. The retrovirus infection spreads at least 4 mm across the septotemporal dentate gyrus axis, illustrations on top of the graph represent the sites of injections (*p < 0.05; ## p < 0.01 compared to chance level). All data shown are mean ± s.e.m. For statistical details, see Table S1.

later, rats were tested in a counterbalanced manner in either context A or B one hour after CNO injection. This design was used to ensure that the order of the context presentation during testing had no influence on subsequent testing. Indeed, we found no differences between the groups whether they were tested first in the conditioning context or the neutral context (data not shown). However, we found that stimulating adult-born neurons increased freezing in conditioning context A as previously found but not in the neutral context B for which the freezing level was very low (<10%; Fig. 7c). These results demonstrate an effect specific to the conditioning context and therefore that stimulation of adult-born neurons does not induce any fear sensitization or generalization but promotes fear memory accuracy. Then, to be sure that adult-born neuron activation was similar when animals were tested in both contexts, rats were killed 90 min after the last test and the expression of Zif268 was analysed in GFP-positive cells. The results showed no differences as the activation was 95.10% in context A and 93.28% in context B (Fig. 7d) indicating the functional recruitment of transduced neurons. By analyzing the density of Zif268-IR cells in the GCL of each group, we found that there was no difference between GFP and Gs-GFP rats, indicating that the stimulation had no impact on GCL activation (Fig. 7e). Finally, we estimated the number of neurons transduced by the Gs-GFP-RV and we found that 2455 ± 43 cells were GFP positive and distributed along the DG septo-temporal axis (Fig. 7f). Altogether, these data demonstrate that stimulating adult-born neurons that were present at the time of learning increases the strength and accuracy of remote contextual fear memory.

4. Discussion

In this study, we first demonstrated that memory quality declines over time. Although rats are very fast to find the position of where the platform was during training, the accurate search of the platform degrades as depicted by the time spent in the target zone, the number of annulus crossing and the Gallagher proximity index. Nevertheless, it could be argued that this loss of accuracy could reflect a change in the strategy employed by the rats to find the platform: as they did not find the platform in the expected location, they tried to find it somewhere else. This could be explained by the fact that spatial memory was generalized over time and that the memory of the precise location of the platform was impaired. Regardless of the spatial strategy used, the decrease of performance appears to reflect a decrease in memory accuracy.

Here, we show that stimulating adult-born neurons generated before learning and independently of their state of maturation at the time of training is a sufficient condition to improve memory accuracy in a navigational task and promote fear response. Our data underline a new role for a population of immature neurons at the time of learning. While this specific population is not activated by learning and not necessary to learn the task and for recent memory retrieval (Lods et al., 2021), they are necessary for remote memory retrieval and for memory maintenance after reactivation (Lods et al., 2021; Snyder et al., 2005). In contrast, the population of adult-born neurons that were mature at the time of learning are involved in spatial memory acquisition (Lemaire et al., 2012) and in recent and remote memory retrieval (Lods et al., 2021; Masachs et al., 2021). When comparing the impact of stimulating neurons that were immature versus mature at the time of training, it seems that the stimulation of mature adult-born neurons is less effective than the stimulation of immature ones. Although the Gallagher index was clearly different between groups, the differences in terms of time spent in zones were not statistically different. Nevertheless, it could also be argued that these differences are rather due to the age of the neurons at the time of retrieval (6 vs 11 weeks) and/or the age of the animals at the time of retrieval (14 vs 19 week-old). However, given that 6 week-old adult born neurons are known to be in the critical phase of enhanced plasticity with a heightened intrinsic excitability and a lower activation threshold (Marin-Burgin et al., 2012; Schmidt-Hieber et al., 2004) and fire at higher rate in vivo (Danielson et al., 2016), they may be more effective in maintaining an accurate memory. Altogether, these results confirm that adult-born neurons are important for consolidation, retrieval and reconsolidation.

The positive effect observed on remote memory seems to be specific to adult-born neurons stimulation. In fact, stimulation of neonatally-generated cells does not improve memory accuracy. It should be noted that more neurons were transduced with the retroviruses in P3 pups than in adult rats, ruling out the hypothesis that the lack of effect observed could be due to a low number of neurons transduced and activated. It also excludes any potential unspecific involvement/recruitment of neighboring cells, i.e. surrounding targeted cells, or global effect of dentate gyrus activation. The results are consistent with previous finding showing that neonatally-generated neurons are not critical for spatial memory (Tronel et al., 2015b), nor for recent (Masachs et al., 2021) or remote retrieval of spatial memories (Lods et al., 2021). Together, these data confirm that neonatally-generated neurons are not involved in processing spatial information in adult rats.

One might question whether adult-born cells have to be young (<6 weeks old) at the time of learning to participate in memory accuracy. We have shown that 3 month-old adult-born neurons are recruited by memory retrieval (Tronel et al., 2015a) and that inhibiting 6 month-old adult-born neurons impairs short-term memory retention, indicating that adult born cells do not need to be young to participate in memory retention (Masachs et al., 2021). Interestingly, 9–12 week-old adult-born neurons lose their ability to promote population sparsity, but become more spatially tuned and can entrain DG principal cells (McHugh et al., 2022), properties that could also support memory accuracy.

Using another hippocampal-dependent task, i.e contextual fear conditioning, we found that stimulating the population of new neurons that was immature at the time of learning specifically enhanced fear response to the conditioning context but not to a neutral context excluding any non-specific fear sensitization and/or generalization. Our data demonstrate that the chemogenetic stimulation of adult-born neurons was specific to the fear-inducing episode and did not simply

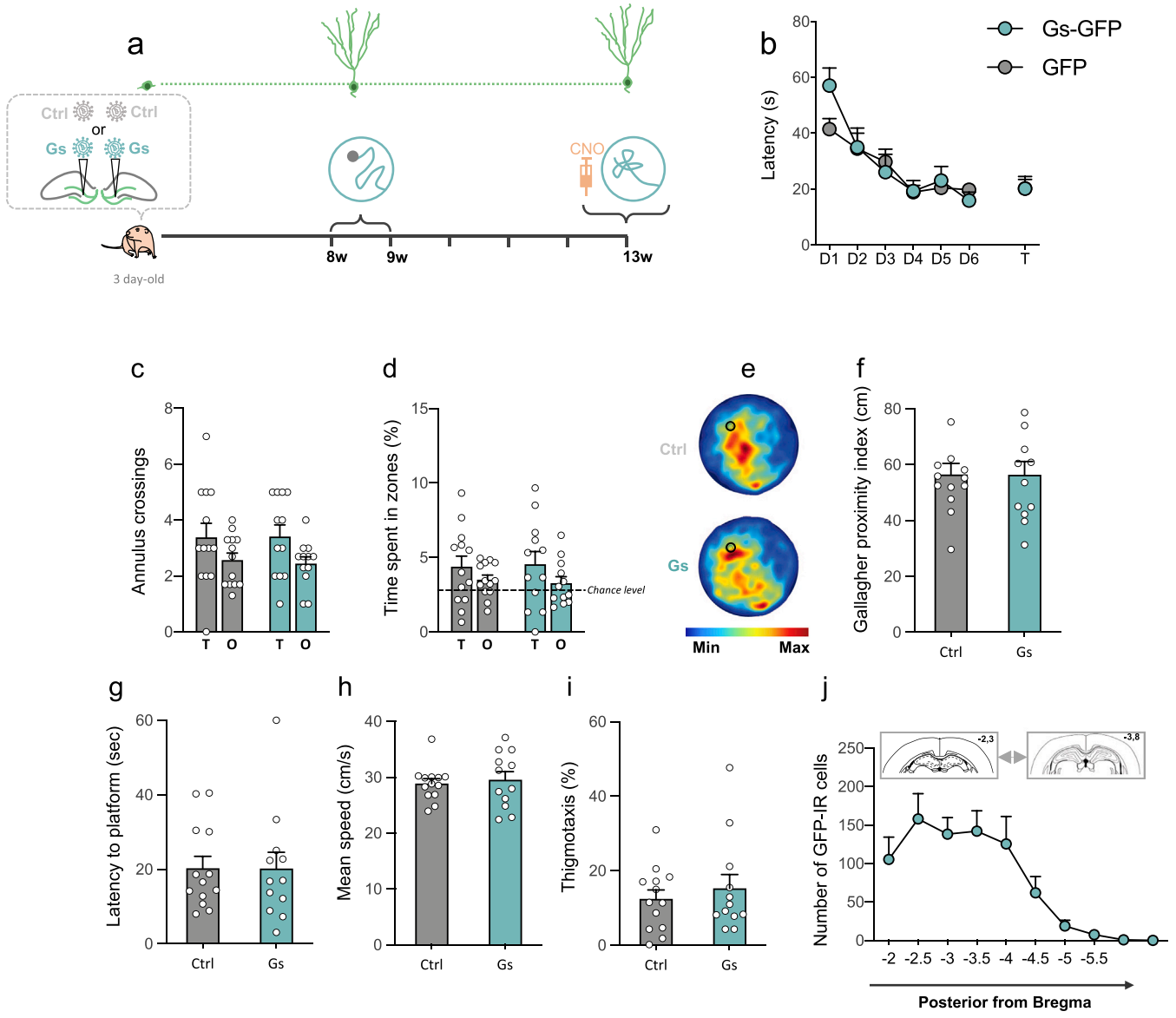

Fig. 5. Chemogenetic stimulation, during remote retention test, of neurons generated during development has no effect on memory. a - Timeline of behavioral procedure with retrovirus injections performed 3 days after birth (Gs-GFP-RV rats, n = 12; GFP-RV rats, n = 13), water maze training 8 weeks after injections and test four weeks after training. CNO was injected 1 h before the test. b – Latency to find the hidden platform: For all groups, latency decreases over time during training and no difference was observed at the retention test. c – Number of annulus crossings during test: there was no difference between groups, with no preference for the TZ. d – Time spent in TZ was not different than the one spent in the other zones for both groups. All time were at chance level (dash line). e - Density plot for grouped data: The black circle represents the position of the platform during training. The color level represents the lowest to the highest location frequency in pixels. f – Gallagher proximity index. There was no difference between groups. g – Latency to cross the platform position. There was no difference between groups. h – Mean Speed of swimming. There was no difference between groups. i – Thigmotaxic behavior. There was no difference between groups. j– Number of GFP-IR in the DG on alternate 1-in-10 50 μm sections. The retrovirus infection spreads at least 4 mm across the septotemporal dentate gyrus axis, illustrations on top of the graph represent the spread of infection. All data shown are mean ± s.e.m. For statistical details, see Table S1.

recall the feeling of fear. This shows that the beneficial effect of adult-born neurons stimulation is not restricted to spatial memory but may be generalized to hippocampal-dependent memory. It would be interesting to address the effect of the stimulation of adult-born neurons already present at the time of learning in other tasks known to be hippocampal- and neurogenesis-dependent (for review see (Abrous et al., 2021b; Koehl and Abrous, 2011)) and to extend our analysis to independent hippocampal tasks.

One could argue that our data are inconsistent with the role of adult-born neurons in active forgetting (Akers et al., 2014; Frankland et al., 2013; Frankland and Josselyn, 2016). Active forgetting refers to, instead of passively disintegrating, unused memories are actively removed (Hardt et al., 2013). This process of clearing is different from the natural fading of the memory trace occurring with the passage of time. It has been shown that "active forgetting" is triggered by the increase of adult born neurons generated in the two weeks *following* training (Akers et al., 2014; Gao et al., 2018). However, these results are not in contradiction with our data because we targeted a population of neurons generated before learning and not after the learning event. Therefore, it is not surprising that active forgetting was not triggered in the present experiments.

One question that remains to be answered is how a selective activation of just a small sample of newborn cells can influence long term memory accuracy? Even though they are few in number, adult-born neurons have a considerable impact on the memory network. Immature neurons have been shown to exhibit higher activity (Danielson

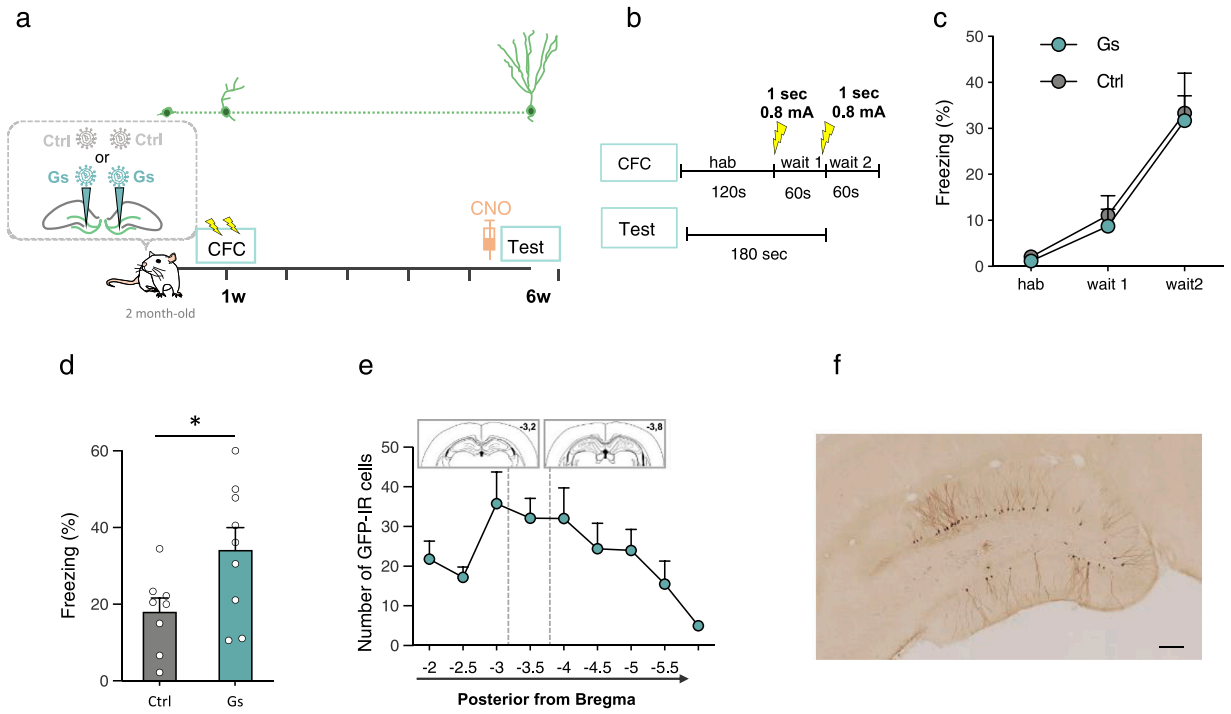

Fig. 6. Chemogenetic stimulation, during remote retention test, of neurons that were immature during CFC improve memory retention. a - Timeline of behavioral procedure with contextual fear conditioning (CFC) 1 week after retrovirus injections (Gs-GFP-RV rats, n = 9; GFP-RV rats, n = 8) and test five weeks after training. CNO was injected 1 h before the test. b- Design of conditioning and test protocol. c - Percentage of freezing during conditioning: there was no freezing difference between the groups. d - Percentage of freezing during test: Gs-GFP rats froze significantly more that control GFP animals (t_{15} =2.30; p = 0.036). e – Number of GFP-IR in the DG on alternate 1-in-10 50 μm sections. The retrovirus infection spreads at least 4 mm across the septotemporal dentate gyrus axis. (*p < 0.05). f - GFP-labeled neurons in DG 6 weeks post-injection of the Gs-GFP-RV (scale: 100 μm). All data shown are mean ± s.e.m. For statistical details, see Table S1.

et al., 2016; McHugh et al., 2022) which may be related to increased excitability, reduced perisomatic inhibition and enhanced synaptic plasticity (long-term depression and excitation) (Lodge and Bischofberger, 2019; Massa et al., 2011). Recently, it has been shown that neurons aged 4–7-weeks support sparser hippocampal population activity, suggesting that sparse coding may allow for higher dimensional network activity in support of memory accuracy (McHugh et al., 2022). In addition, they control network oscillations (Lacefield et al., 2012; McHugh et al., 2022) most probably via inhibitory interneurons (Drew et al., 2016; Lodge and Bischofberger, 2019; Park et al., 2015; Temprana et al., 2015). By modulating the temporal dynamics of hippocampal network activity they could exert their influence beyond hippocampal activity (Mateus-Pinheiro et al., 2021). In our experiments, we did not find any effect of the chemogenetic stimulation of adult-born neurons on the activity of granular cell layer of the DG. These results are in agreement with some previous data (Temprana et al., 2015) but not with others describing a decrease in DG activity after optogenetic stimulation of a cohort of young adult-born neurons (Drew et al., 2016). This discrepancy between our study (and that of Drew et al.) could be explained by the fact that, in their experiment, they targeted a cohort of adult-born neurons aged 0–6 weeks, and therefore a much higher cell number. It is unlikely that the stimulation of a cohort of adult-born neurons generated over one day induces the same effect than the stimulation of neurons generated over the last 6 weeks. An alternative hypothesis is that IEG analysis does not capture the fine transient dynamic changes that can be observed using calcium imaging.

How do adult-born participate to the retrieval of remote memory trace is also an unresolved issue. According to a recent definition (Josselyn and Tonegawa, 2020), “engram cells” are: i) activated by a learning experience, ii) physically or chemically modified by the learning experience, and iii) reactivated by subsequent presentation of the stimuli present at the learning experience, resulting in memory retrieval. Mature adult-born neurons fulfill all these criteria whereas neonatally born neurons do not. The situation is more complex for immature neurons. We have previously shown that dendritic development and spinogenesis of this population is increased by spatial learning (Tronel et al., 2010a), fulfilling criteria ii). Furthermore, we reported that this population is activated by remote retrieval (Lods et al., 2021) and the present results demonstrate that activation of these neurons leads to the reengagement of the network and eventually to memory retrieval, fulfilling criteria iii). However, this immature population is not activated by learning, corresponding to the first criteria, using c-Fos and Zif268 as a proxy of neuronal activity (Lods et al., 2021; Masachs et al., 2021; Snyder et al., 2009). However it has recently been shown that the lack of expression of cFos cannot be taken as evidence for the absence of activity (Lee et al., 2021) and that other markers such as pCREB are expressed in immature neurons (Jungenitz et al., 2014) suggesting that immature adult-born cells could still fulfill all the criteria of engram cells. Furthermore, the fact that remote memory cannot be retrieved accurately through natural cues but only artificially through stimulation of immature adult-born neurons suggests that this population could represent “silent engram cells” (Roy et al., 2017), especially in the case of contextual memory where the hippocampal engram slowly becomes silent over time. It should be noted that their stimulation does not increase freezing in a neutral context, which is different from what was previously reported for silent engram cells studies (Guskjolen et al., 2018; Kitamura et al., 2017; Ryan et al., 2015). However, in contrast to our study, silent engram cells in these previous studies were mature at the time of encoding. It is therefore possible that experience during the critical period of maturation influences neurons in a way that, when they become mature, their activity specifically responds to the previously experienced events (Tashiro et al., 2007; Trouche et al., 2009). Interestingly, since immature adult-born neurons do not seem to be necessary for learning (Lemaire et al., 2012), they could be primed by learning as previously suggested (Alvarez et al., 2016) and their connections were expanded by learning. Therefore, they would be more

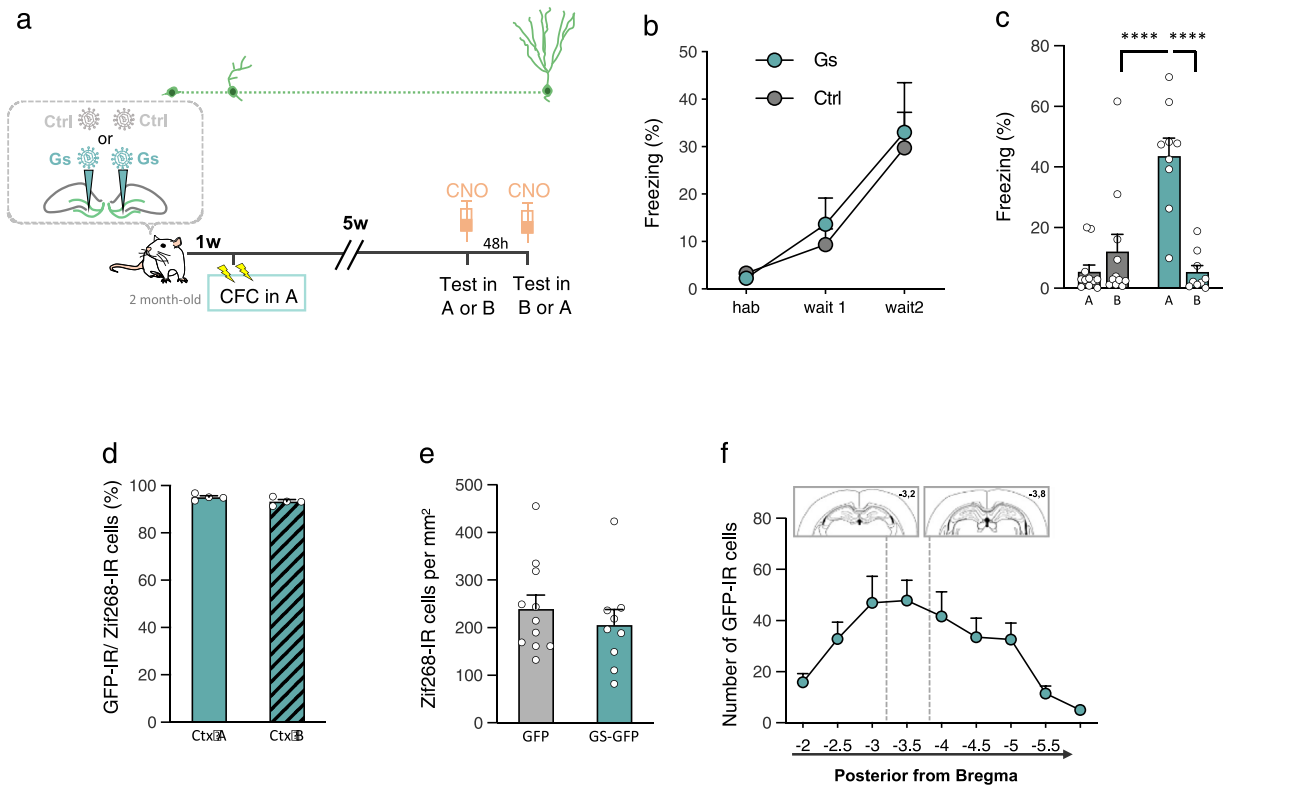

Fig. 7. Memory improvement induced by chemogenetic stimulation of neurons that were immature during CFC is specific to the conditioning context. a - Timeline of behavioral procedure with contextual fear conditioning (CFC) 1 week after retrovirus injections (Gs-GFP-RV rats, n = 9; GFP-RV rats, n = 11) and test five weeks after training. Half of the rats was tested first in context A and then in context B 48 h later, the other half was tested first in B and then in A. CNO was injected 1 h before each test. b - Percentage of freezing during conditioning: there was no freezing difference between the groups. c - Percentage of freezing tests: Gs-GFP rats froze significantly more in ctx A than in ctx B and more than control GFP animals in context A. No differences were observed for control GFP rats (context X group interaction: $F(1,18)= 34.19$; $p < 0.0001$). d – Zif268 expression in GFP-IR cells. Percentage of expression was similar between both contexts. e -Number of Zif268-IR cells par mm^2 in the DG. There was no difference between rats injected with the GFP-RV or the Gs-GFP-RV. f-Number of GFP-IR in the DG on alternate 1-in-10 50 μm sections. The retrovirus infection spreads at least 4 mm across the septotemporal dentate gyrus axis. (*$p < 0.05$). All data shown are mean ± s.e.m. For statistical details, see Table S1.

prone to be involved in the maintenance of the memory trace. In addition, further experiments are necessary to determine how immature neurons could, together with the mature adult-born neurons, be engaged in the engram network. It could be proposed that memory engrams could be functionally heterogeneous (Sun et al., 2020) and that immature and mature adult-born neuronal subpopulations could encode distinct aspects of the memory by engaging distinct synaptic and circuit mechanisms. Finally, our data support the hypothesis that even if they are not fully integrated into the hippocampal network at the age of 1–2 weeks, these adult-born neurons will eventually become important for memory (Shors et al., 2001). Indeed, we have previously shown that, in adults, spatial learning accelerates spine maturation of 1–2 week old neurons (Tronel et al., 2010b) and synaptically driven action potential firing have been found in adult-born neurons as soon as 1.5 weeks (Heigele et al., 2016). Together, these data suggest that synaptic inputs at the time of spine formation may promote specific connections between immature neurons (1–2 weeks old) and mature neurons which, as suggested by (Zhao et al., 2006), may allow these immature adult-born neurons to be involved in the hippocampal network supporting memory formation and/or expression even before the synapses are optimally formed on spines. In summary, these findings promote the idea that adult neurogenesis is essential for memory accuracy (Yu et al., 2019) and could be a valuable tool to compensate for the loss of precision and detail induced by the passage of time. Since the dentate gyrus is known to govern the reactivation of remote memory trace (Ryan and Tonegawa, 2016) and to diminish generalization of remote fear memories (Guo et al., 2018), our results confirm that adult-born dentate neurons are key players in the role of the dentate network. Promoting memory is a relevant outcome when it comes to aging and stress. During aging, not only the rate but also the responsiveness of adult hippocampal neurogenesis is altered (Drapeau and Abrous, 2008; Montaron et al., 2020). In the context of stress and in particular in post-traumatic stress disorders, it would be of interest to determine whether the manipulation of adult-born neurons could alleviate maladaptive memories. Recently, chemogenetic treatments have been proposed in humans (Lieb et al., 2019), suggesting that manipulating the activity of adult-born neurons could be a promising strategy for prevention or treatment of memory loss.

Funding

This work was supported by INSERM (to DNA) and the ANR (to ST ANR-16-CE37-0018-01; to DC ANR-13-BSV4-0006-01) and by the Université de Bordeaux. ML was supported by a MESR (Ministère de l'Enseignement Supérieur et de la Recherche) fellowship and by the ANR (ANR-16-CE37-0018-01). NM was supported by the ANR (ANR-16-CE37-0018-01) and by the Fondation Fyssen. PM was supported by the FRC (to DNA). This work benefited from the support of the Biochemistry and Biophysics Facility of the Bordeaux Neurocampus, funded by the LabEX BRAIN ANR-10-LABX-43 and the Animal Housing facility funded by INSERM and LabEX BRAIN ANR-10-LABX-43. The confocal analysis was done in the Bordeaux Imaging Center (BIC), a service unit of the CNRS-INSERM and Bordeaux University, member of the national infrastructure France BioImaging supported by the French National

Research Agency (ANR-10-INBS-04).

Data availability

All data supporting the findings of this study are provided within the paper and its supplementary information. A source data file is provided with this paper. The CAG-Gs-IRES-GFP retroviral construct is available upon request to the authors after MTA approval. All additional information will be made available upon reasonable request to the authors.

Acknowledgments

We thank Dr Fred Gage and Dr Dieter Chichung Lie for providing the retroviral vector CAG–GFP and the 293GPG cell line, respectively. We gratefully acknowledge Cedric Dupuy for animal care. The help of BIC engineer, Monica Fernandez Monreal is acknowledged.

Author contributions

ML designed and performed the experiments and analyzed the data. PM performed the experiments. EP designed the retroviruses. FF produced the retroviruses. GT, WM and VC performed the electrophysiological experiments. DC supervised electrophysiological experiments and revised the paper. GF designed the experiments and revised the paper. DNA conceived experiments and wrote the paper. ST conceived and designed the experiments, performed experiments, analyzed the data and wrote the paper. All the authors edited and approved the final version of the manuscript.

Competing interests

The authors declare no competing interests.

Appendix A. Supplementary material

Supplementary data associated with this article can be found in the online version at doi:10.1016/j.pneurobio.2022.102364.

References

Abrous, D.N., Koehl, M., Lemoine, M., 2021a. A Baldwin interpretation of adult hippocampal neurogenesis: from functional relevance to physiopathology. Mol. Psychiatry. https://doi.org/10.1038/s41380-021-01172-4.

Abrous, D.N., Koehl, M., Lemoine, M., 2021b. A Baldwin interpretation of adult hippocampal neurogenesis: from functional relevance to physiopathology. Mol. Psychiatry. https://doi.org/10.1038/s41380-021-01172-4.

Akers, K.G., Martinez-Canabal, A., Restivo, L., Yiu, A.P., De Cristofaro, A., Hsiang, H.L., Wheeler, A.L., Guskjolen, A., Niibori, Y., Shoji, H., Ohira, K., Richards, B.A., Miyakawa, T., Josselyn, S.A., Frankland, P.W., 2014. Hippocampal neurogenesis regulates forgetting during adulthood and infancy. Science 344, 598–602. https://doi.org/10.1126/science.1248903.

Alvarez, D.D., Giacomini, D., Yang, S.M., Trinchero, M.F., Temprana, S.G., Buttner, K.A., Beltramone, N., Schinder, A.F., 2016. A disynaptic feedback network activated by experience promotes the integration of new granule cells. Science 354, 459–465. https://doi.org/10.1126/science.aaf2156.

Armbruster, B., Brandeau, M.L., 2007. Contact tracing to control infectious disease: when enough is enough. Health Care Manag. Sci. 10, 341–355. https://doi.org/10.1007/s10729-007-9027-6.

Arruda-Carvalho, M., Sakaguchi, M., Akers, K.G., Josselyn, S.A., Frankland, P.W., 2011. Posttraining ablation of adult-generated neurons degrades previously acquired memories. J. Neurosci. 31, 15113–15127. https://doi.org/10.1523/JNEUROSCI.3432-11.2011.

Berdugo-Vega, G., Arias-Gil, G., L ias-Gilegaorg, A., Artegiani, B., Wasielewska, J.M., Lee, C.-C., Lippert, M.T., Kempermann, G., Takagaki, K., Calegari, F., 2020. Increasing neurogenesis refines hippocampal activity rejuvenating navigational learning strategies and contextual memory throughout life. Nat. Commun. 11, 135. https://doi.org/10.1038/s41467-019-14026-z.

Cole, J.D., Espinueva, D.F., Seib, D.R., Ash, A.M., Cooke, M.B., Cahill, S.P., O P.lle, T.P., Kwan, S.S., Snyder, J.S., 2020. Adult-born hippocampal neurons undergo extended development and are morphologically distinct from neonatally-born neurons. J. Neurosci. 40, 5740–5756. https://doi.org/10.1523/JNEUROSCI.1665-19.2020.

Danielson, N.B., Kaifosh, P., Zaremba, J.D., Lovett-Barron, M., Tsai, J., Denny, C.A., Balough, E.M., Goldberg, A.R., Drew, L.J., Hen, R., Losonczy, A., Kheirbek, M.A., 2016. Distinct contribution of adult-born hippocampal granule cells to context encoding. Neuron 90, 101–112. https://doi.org/10.1016/j.neuron.2016.02.019.

Deng, W., Aimone, J.B., Gage, F.H., 2010. New neurons and new memories: how does adult hippocampal neurogenesis affect learning and memory. Nat. Rev. Neurosci. 11, 339–350. https://doi.org/10.1038/nrn2822.

Drapeau, E., Abrous, N.D., 2008. Role of neurogenesis in age-related memory disorders. Aging Cell.

Drew, L.J., Kheirbek, M.A., Luna, V.M., Denny, C.A., Cloidt, M.A., Wu, M.V., Jain, S., Scharfman, H.E., Hen, R., 2016. Activation of local inhibitory circuits in the dentate gyrus by adult-born neurons. Hippocampus 26, 763–778. https://doi.org/10.1002/hipo.22557.

Dupret, D., Fabre, A., Dobrossy, M.D., Panatier, A., Rodriguez, J.J., Lamarque, S., Lemaire, V., Oliet, S.H., Piazza, P.V., Abrous, D.N., 2007. Spatial learning depends on both the addition and removal of new hippocampal neurons. PLoS Biol. 5, e214.

Fanselow, M.S., 1990. Factors governing one-trial contextual conditioning. Anim. Learn. Behav. 18, 264–270. https://doi.org/10.3758/BF03205285.

Fanselow, M.S., 2000. Contextual fear, gestalt memories, and the hippocampus. Behav. Brain Res. 110, 73–81. https://doi.org/10.1016/S0166-4328(99)00186-2.

Frankland, P.W., Josselyn, S.A., 2016. Hippocampal neurogenesis and memory clearance. Neuropsychopharmacology 41, 382–383. https://doi.org/10.1038/npp.2015.243.

Frankland, P.W., K W.kl, S., Josselyn, S.A., 2013. Hippocampal neurogenesis and forgetting. Trends Neurosci. 36, 497–503. https://doi.org/10.1016/j.tins.2013.05.002.

Gallagher, M., Burwell, R., Burchinal, M., 1993. Severity of spatial learning impairment in aging: development of a learning index for performance in the Morris water maze. Behav. Neurosci. 107, 618–626. https://doi.org/10.1037//0735-7044.107.4.618.

Gao, A., Xia, F., Guskjolen, A.J., Ramsaran, A.I., Santoro, A., Josselyn, S.A., Frankland, P.W., 2018. Elevation of hippocampal neurogenesis induces a temporally graded pattern of forgetting of contextual fear memories. J. Neurosci. 38, 3190–3198. https://doi.org/10.1523/JNEUROSCI.3126-17.2018.

Goncalves, J.T., Schafer, S.T., Gage, F.H., 2016. Adult neurogenesis in the hippocampus: from stem cells to behavior. Cell 167, 897–914. https://doi.org/10.1016/j.cell.2016.10.021.

Gu, Y., Arruda-Carvalho, M., Wang, J., Janoschka, S.R., Josselyn, S.A., Frankland, P.W., Ge, S., 2012. Optical controlling reveals time-dependent roles for adult-born dentate granule cells. Nat. Neurosci. 15, 1700–1706. https://doi.org/10.1038/nn.3260.

Guo, N., Soden, M.E., Herber, C., Kim, M.T., Besnard, A., Lin, P., Ma, X., Cepko, C.L., Zweifel, L.S., Sahay, A., 2018. Dentate granule cell recruitment of feedforward inhibition governs engram maintenance and remote memory generalization. Nat. Med. 24, 438–449. https://doi.org/10.1038/nm.4491.

Guskjolen, A., Kenney, J.W., de la Parra, J., Yeung, B.A., Josselyn, S.A., Frankland, P.W., 2018. Recovery of org/10.1038/nm.4491t of feedfo. e3 Curr. Biol. 28, 2283–2290. https://doi.org/10.1016/j.cub.2018.05.059.

Hardt, O., Nader, K., Nadel, L., 2013. Decay happens: the role of active forgetting in memory. Trends Cogn. Sci. 17, 111–120. https://doi.org/10.1016/j.tics.2013.01.001.

Heigele, S., Sultan, S., Toni, N., Bischofberger, J., 2016. Bidirectional GABAergic control of action potential firing in newborn hippocampal granule cells. Nat. Neurosci. 19, 263–270. https://doi.org/10.1038/nn.4218.

Jessberger, S., Aigner, S., Clemenson, G.D., Toni, N., Lie, D.C., Karalay, O., Overall, R., Kempermann, G., Gage, F.H., 2008. Cdk5 regulates accurate maturation of newborn granule cells in the adult hippocampus. PLoS Biol. 6, e272 https://doi.org/10.1371/journal.pbio.0060272.

Josselyn, S.A., Tonegawa, S., 2020. Memory engrams: recalling the past and imagining the future. Science 367, eaaw4325. https://doi.org/10.1126/science.aaw4325.

Jungenitz, T., Radic, T., Jedlicka, P., Schwarzacher, S.W., 2014. High-frequency stimulation induces gradual immediate early gene expression in maturing adult-generated hippocampal granule cells. Cereb. Cortex 24, 1845–1857. https://doi.org/10.1093/cercor/bht035.

Kitamura, T., Ogawa, S.K., Roy, D.S., Okuyama, T., Morrissey, M.D., Smith, L.M., Redondo, R.L., Tonegawa, S., 2017. Engrams and circuits crucial for systems consolidation of a memory. Science 356, 73–78. https://doi.org/10.1126/science.aam6808.

Koehl, M., Abrous, D.N., 2011. A new chapter in the field of memory: adult hippocampal neurogenesis. Eur. J. Neurosci. 33, 1101–1114. https://doi.org/10.1111/j.1460-9568.2011.07609.x.

Lacefield, C.O., Itskov, V., Reardon, T., Hen, R., Gordon, J.A., 2012. Effects of adult-generated granule cells on coordinated network activity in the dentate gyrus. Hippocampus 22, 106–116. https://doi.org/10.1002/hipo.20860.

Lee, J., Urban-Ciecko, J., Park, E., Zhu, M., Myal, S.E., Margolis, D.J., Barth, A.L., 2021. FosGFP expression does not capture a sensory learning-related engram in superficial layers of mouse barrel cortex. Proc. Natl. Acad. Sci. USA 118, e2112212118. https://doi.org/10.1073/pnas.2112212118.

Lemaire, V., Tronel, S., Montaron, M.F., Fabre, A., Dugast, E., Abrous, D.N., 2012. Long-lasting plasticity of hippocampal adult-born neurons. J. Neurosci. Off. J. Soc. Neurosci. 32, 3101–3108. https://doi.org/10.1523/JNEUROSCI.4731-11.2012.

Lieb, A., Weston, M., Kullmann, D.M., 2019. Designer receptor technology for the treatment of epilepsy. eBioMedicine 43, 641–649. https://doi.org/10.1016/j.ebiom.2019.04.059.

Lodge, M., Bischofberger, J., 2019. Synaptic properties of newly generated granule cells support sparse coding in the adult hippocampus. Behav. Brain Res. 372, 112036 https://doi.org/10.1016/j.bbr.2019.112036.

Lods, M., Pacary, E., Mazier, W., Farrugia, F., Mortessagne, P., Masachs, N., Charrier, V., Massa, F., Cota, D., Ferreira, G., Abrous, D.N., Tronel, S., 2021. Adult-born neurons

immature during learning are necessary for remote memory reconsolidation in rats. Nat. Commun. 12, 1778. https://doi.org/10.1038/s41467-021-22069-4.
Madroronal, N., Delgado-Garcor, J.M., Fernado-Garcorg/, A., Chatterjee, J., K at, M., Mattucci, C., Jain, A., Tsetsenis, T., Illarionova, A., Grinevich, V., Gross, C.T., Gruart, A., 2016. Rapid erasure of hippocampal memory following inhibition of dentate gyrus granule cells. Nat. Commun. 7, 10923. https://doi.org/10.1038/ncomms10923.
Marin-Burgin, A., Mongiat, L.A., Pardi, M.B., Schinder, A.F., 2012. Unique processing during a period of high excitation/inhibition balance in adult-born neurons. Science 335, 1238–1242. https://doi.org/10.1126/science.1214956.
Masachs, N., Charrier, V., Farrugia, F., Lemaire, V., Blin, N., Mazier, W., Tronel, S., Montaron, M.-F., Ge, S., Marsicano, G., Cota, D., Deroche-Gamonet, V., Herry, C., Abrous, D.N., 2021. The temporal origin of dentate granule neurons dictates their role in spatial memory. Mol. Psychiatry 26, 7130–7140. https://doi.org/10.1038/s41380-021-01276-x.
Massa, F., Koehl, M., Koelh, M., Wiesner, T., Grosjean, N., Revest, J.-M., Piazza, P.-V., Abrous, D.N., Oliet, S.H.R., 2011. Conditional reduction of adult neurogenesis impairs bidirectional hippocampal synaptic plasticity. Proc. Natl. Acad. Sci. USA 108, 6644–6649. https://doi.org/10.1073/pnas.1016928108.
Mateus-Pinheiro, A., Patrus-P, P., Alves, N.D., Martins-Macedo, J., Caetano, I., Silveira-Rosa, T., Aravei, B., Mateus-Pinheiro, M., Silva-Correia, J., Sardinha, V.M., Loureiro-Campos, E., Rodrigues, A.J., Oliveira, J.F., Bessa, J.M., Sousa, N., Pinto, L., 2021. Hippocampal cytogenesis abrogation impairs inter-regional communication between the hippocampus and prefrontal cortex and promotes the time-dependent manifestation of emotional and cognitive deficits. Mol. Psychiatry. https://doi.org/10.1038/s41380-021-01287-8.
McAvoy, K.M., Scobie, K.N., Berger, S., Russo, C., Guo, N., Decharatanachart, P., Vega-Ramirez, H., Miake-Lye, S., Whalen, M., Nelson, M., Bergami, M., Bartsch, D., Hen, R., Berninger, B., Sahay, A., 2016. Modulating neuronal competition dynamics in the dentate gyrus to rejuvenate aging memory circuits. Neuron 91, 1356–1373. https://doi.org/10.1016/j.neuron.2016.08.009.
McHugh, S.B., Lopes-Dos-Santos, V., Gava, G.P., Hartwich, K., Tam, S.K.E., Bannerman, D.M., Dupret, D., 2022. Adult-born dentate granule cells promote hippocampal population sparsity. Nat. Neurosci. https://doi.org/10.1038/s41593-022-01176-5.
Miller, S.M., Sahay, A., 2019. Functions of adult-born neurons in hippocampal memory interference and indexing. Nat. Neurosci. https://doi.org/10.1038/s41593-019-0484-2.
Montaron, M.-F., Charrier, V., Blin, N., Garcia, P., Abrous, D.N., 2020. Responsiveness of dentate neurons generated throughout adult life is associated with resilience to cognitive aging. Aging Cell 19, e13161. https://doi.org/10.1111/acel.13161.
Moser, E.I., Krobert, K.A., Moser, M.B., Morris, R.G., 1998. Impaired spatial learning after saturation of long-term potentiation. Science 281, 2038–2042. https://doi.org/10.1126/science.281.5385.2038.
Ory, D.S., Neugeboren, B.A., Mulligan, R.C., 1996. A stable human-derived packaging cell line for production of high titer retrovirus/vesicular stomatitis virus G pseudotypes. Proc. Natl. Acad. Sci. USA 93, 11400–11406. https://doi.org/10.1073/pnas.93.21.11400.
Park, E.H., Burghardt, N.S., Dvorak, D., Hen, R., Fenton, A.A., 2015. Experience-dependent regulation of dentate gyrus excitability by adult-born granule cells. J. Neurosci. 35, 11656–11666. https://doi.org/10.1523/JNEUROSCI.0885-15.2015.
Pignatelli, M., Ryan, T.J., Roy, D.S., Lovett, C., Smith, L.M., Muralidhar, S., Tonegawa, S., 2019. Engram cell excitability state determines the efficacy of memory retrieval. e5 Neuron 101, 274–284. https://doi.org/10.1016/j.neuron.2018.11.029.
Roy, D.S., Muralidhar, S., Smith, L.M., Tonegawa, S., 2017. Silent memory engrams as the basis for retrograde amnesia. Proc. Natl. Acad. Sci. USA 114, E9972. https://doi.org/10.1073/pnas.1714248114.
Ryan, T.J., Tonegawa, S., 2016. Rehebbilitating memory. Neuropsychopharmacology 41, 1437. https://doi.org/10.1038/npp.2016.4.
Ryan, T.J., Roy, D.S., Pignatelli, M., Arons, A., Tonegawa, S., 2015. Memory. Engram cells retain memory under retrograde amnesia. Science 348, 1007–1013. https://doi.org/10.1126/science.aaa5542.
Sahay, A., Scobie, K.N., Hill, A.S., O S.ie//d, C.M., Kheirbek, M.A., Burghardt, N.S., Fenton, A.A., Dranovsky, A., Hen, R., 2011. Increasing adult hippocampal neurogenesis is sufficient to improve pattern separation. Nature 472, 466–470. https://doi.org/10.1038/nature09817.
Schmidt-Hieber, C., Jonas, P., Bischofberger, J., 2004. Enhanced synaptic plasticity in newly generated granule cells of the adult hippocampus. Nature 429, 184–187. https://doi.org/10.1038/nature02553.
Shors, T.J., Miesegaes, G., Beylin, A., Zhao, M., Rydel, T., Gould, E., 2001. Neurogenesis in the adult is involved in the formation of trace memories. Nature 410, 372–376.
Snyder, J.S., Hong, N.S., McDonald, R.J., Wojtowicz, J.M., 2005. A role for adult neurogenesis in spatial long-term memory. Neuroscience 130, 843–852.
Snyder, J.S., Choe, J.S., Clifford, M.A., Jeurling, S.I., Hurley, P., Brown, A., Kamhi, J.F., Cameron, H.A., 2009. Adult-born hippocampal neurons are more numerous, faster maturing, and more involved in behavior in rats than in mice. J. Neurosci. 29, 14484–14495.
Sun, X., Bernstein, M.J., Meng, M., Rao, S., S ogstei, A.T., Yao, L., Zhang, X., Anikeeva, P. O., Lin, Y., 2020. Functionally distinct neuronal ensembles within the memory engram. Cell 181 (410–423), e17. https://doi.org/10.1016/j.cell.2020.02.055.
Tashiro, A., Makino, H., Gage, F.H., 2007. Experience-specific functional modification of the dentate gyrus through adult neurogenesis: a critical period during an immature stage. The Journal of neuroscience : the official journal of the Society for Neuroscience 27, 3252–3259. https://doi.org/10.1523/JNEUROSCI.4941-06.2007.
Tayler, K.K., Tanaka, K.Z., Reijmers, L.G., Wiltgen, B.J., 2013. Reactivation of neural ensembles during the retrieval of recent and remote memory. Curr. Biol. 23, 99–106. https://doi.org/10.1016/j.cub.2012.11.019.
Temprana, S.G., Mongiat, L.A., Yang, S.M., Trinchero, M.F., Alvarez, D.D., Kropff, E., Giacomini, D., Beltramone, N., Lanuza, G.M., Schinder, A.F., 2015. Delayed coupling to feedback inhibition during a critical period for the integration of adult-born granule cells. Neuron 85, 116–130. https://doi.org/10.1016/j.neuron.2014.11.023.
Tronel, S., Fabre, A., Charrier, V., Oliet, S.H., Gage, F.H., Abrous, D.N., 2010a. Spatial learning sculpts the dendritic arbor of adult-born hippocampal neurons. Proc. Natl. Acad. Sci. USA 107, 7963–7968. https://doi.org/10.1073/pnas.0914613107.
Tronel, S., Fabre, A., Charrier, V., Oliet, S.H., Gage, F.H., Abrous, D.N., 2010b. Spatial learning sculpts the dendritic arbor of adult-born hippocampal neurons. Proc. Natl. Acad. Sci. USA 107, 7963–7968. https://doi.org/10.1073/pnas.0914613107.
Tronel, S., Charrier, V., Sage, C., Maitre, M., Leste-Lasserre, T., Abrous, D.N., 2015a. Adult-born dentate neurons are recruited in both spatial memory encoding and retrieval. Hippocampus 25, 1472–1479. https://doi.org/10.1002/hipo.22468.
Tronel, S., Lemaire, V., Charrier, V., Montaron, M.F., Abrous, D.N., 2015b. Influence of ontogenetic age on the role of dentate granule neurons. Brain Struct. Funct. 220, 645–661. https://doi.org/10.1007/s00429-014-0715-y.
Trouche, S., Bontempi, B., Roullet, P., Rampon, C., 2009. Recruitment of adult-generated neurons into functional hippocampal networks contributes to updating and strengthening of spatial memory. Proc. Natl. Acad. Sci. USA 106, 5919–5924. https://doi.org/10.1073/pnas.0811054106.
Yu, R.Q., Cooke, M., Seib, D.R., Zhao, J., Snyder, J.S., 2019. Adult neurogenesis promotes efficient, nonspecific search strategies in a spatial alternation water maze task. Behav. Brain Res. 376, 112151 https://doi.org/10.1016/j.bbr.2019.112151.
Zhao, C., Teng, E.M., Summers, R.G., Ming, G.L., Gage, F.H., 2006. Distinct morphological stages of dentate granule neuron maturation in the adult mouse hippocampus. J. Neurosci. 26, 3–11.